

Coefficient of restitution for bouncing nanoparticles

A. I. Ayesh,^{1,*} S. A. Brown,¹ A. Awasthi,² S. C. Hendy,^{2,3} P. Y. Convers,¹ and K. Nichol¹

¹*MacDiarmid Institute for Advanced Materials and Nanotechnology, Department of Physics and Astronomy, University of Canterbury, Christchurch, New Zealand*

²*Industrial Research Ltd., Lower Hutt 5040, New Zealand*

³*MacDiarmid Institute for Advanced Materials and Nanotechnology, Victoria University of Wellington, Wellington 6140, New Zealand*

(Received 21 January 2010; published 17 May 2010)

We demonstrate the measurement of the coefficient of restitution, e , for nanoparticles, through observations of the final distribution of bismuth particles that have bounced within silicon V-grooves. The experiments, taken together with complementary molecular-dynamics simulations, show that e is generally smaller for liquid than for solid nanoparticles, and that macroscopic theories underestimate the velocity dependence of e . Hence, while nanoparticles are harder than bulk materials, once they have begun to yield the rate of increase of the inelastic deformation is greater.

DOI: [10.1103/PhysRevB.81.195422](https://doi.org/10.1103/PhysRevB.81.195422)

PACS number(s): 62.25.-g, 61.46.Bc, 62.20.F-

I. INTRODUCTION

Many of the observable properties of macroscopic everyday objects are governed by their elastic and mechanical materials properties. For example, balls bounce when incident on surfaces, such as cricket pitches or walls, because of the elasticity of the materials involved. The elastomechanical properties of nanoparticles can, however, be quite different to those of their macroscopic counterparts. Nanoparticles have been found to exhibit an increase in stiffness¹ and yield stress^{2,3} but because of a tendency to adhere to surfaces,⁴ experimental observations of bouncing are rare.⁵⁻⁷ Hence experimental studies (see Refs. 4 and 8 for reviews) of nanoparticle impacts have focused on implantation,⁹ and deformation, adhesion, and soft landing.¹⁰

Bouncing is usually characterized by the coefficient of restitution, e , which is the ratio of the final and the incident velocities, v_f/v_0 , but there are no known measurements of e for nanoparticles. This is surprising since e reflects the elastomechanical properties of the particles and is an important parameter in areas ranging from granular flows to polishing of semiconductor wafers to filtration.¹¹ The latter is particularly important since nanoparticles may present significant health and safety issues,¹² and for small particles, thermal velocities, when combined with large e , could lead to penetration of personal protection filters.¹³

It has recently been shown that nanoparticles incident on a V-shaped template etched into a silicon wafer can be made to assemble into nanowires, and that the assembly is due to bouncing of the particles.⁵ Here we extend previous experiments⁵ and molecular-dynamics (MD) simulations³ to investigate the coefficient of restitution during the bouncing process. Specifically, we report measurements of the coefficient of restitution for ~ 30 nm Bi nanoparticles incident on etched silicon surfaces together with complementary molecular-dynamics simulations of nanoparticles undergoing bouncing at oblique angles. We obtain different values of e for liquid and solid nanoparticles, and show that for solid particles, the variation in e with v_0 is much stronger than expected from macroscopic theory,¹⁴ due to strong plastic deformation³ during the collision. The inelastic deformation

of the liquid particles (plasticity is a property of solids) has a similar velocity dependence.

II. EXPERIMENTAL

The nanoparticles (or “clusters”) are generated in an inert-gas aggregation (IGA) source¹⁵ by evaporation of metal from a crucible into a cool inert-gas stream and deposited inside an ultrahigh-vacuum compatible deposition chamber.¹⁵ Particle size and velocity are controlled by the crucible temperature (T_c), gas flow rate (f), inert-gas pressure (P_s), type of inert gas, and temperature of the source (T_s).¹⁵ In the present experiments, Bi was evaporated with T_c between 970 and 1170 K into either argon gas or a Ar/He mixture ($f = 45\text{--}210$ sccm) which is nominally at the temperature of the walls of the source ($T_s = 77$ or 290 K). The bismuth clusters formed have average diameters ranging from 20 to 40 nm depending on the source conditions (T_c, T_s, f) and are deposited onto etched silicon substrates which are held at a temperature T_{sub} .

III. EXPERIMENTAL RESULTS

Figure 1 shows schematically the deposition of bismuth nanoparticles into the V-shaped templates. Scanning electron microscope (SEM) images (see Fig. 2) show that, while deposited uniformly, nanoparticles with high velocities are not distributed uniformly after deposition. The nanoparticles are almost completely absent from the upper walls of the V-grooves, and accumulate near the apex of the V-groove [Figs. 2(a) and 2(b)]. Obviously the particles do not stick at their first point of impact.

In both Figs. 2(a) and 2(b), where the mean deposited thicknesses are ~ 2 nm and ~ 7 nm, respectively, it is clear that there is a well-defined edge to the distribution of deposited particles (solid red lines). The well-defined edges of the cluster distribution, and the stacking of clusters on top of each other, come about because particles bounce from the opposite face of the V-groove (see Fig. 1). At high coverages [Fig. 2(b)], clusters landing on other clusters (which had arrived previously) tend to “avalanche” toward the apex and so

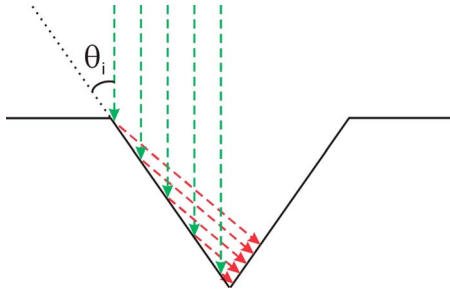


FIG. 1. (Color online) Schematic of the particle bouncing process. Particles are incident normal to the surface of the silicon wafer, which results in an angle of incidence $\theta_i=35^\circ$ relative to the surface of V-grooves etched into the wafer. (This angle is defined by the angle between the (100) and (111) planes of Si—see Ref. 5.) The particles bounce from one face of the V-groove (reflection angle θ_r) and adhere to the opposite face. When the sample is tilted, the angle of incidence of the particles is different for the two sides of the V-groove, and the width of the particle distribution on the opposite face can be used to determine θ_r as a function of θ_i .

we focus on determination of the bouncing angle from low-coverage depositions.

Figure 1 shows the angle of incidence, measured relative to the V-groove wall, is $\theta_i=35^\circ$ and that a well-defined edge can only exist if the particles bounce once¹⁶ at a relatively well-defined angle, θ_r . The width of the nanoparticle distribution in the V-groove, together with the width of the V-groove (typically 2–4 μm), can then be used to calculate θ_r [$\sim 15^\circ$ in Figs. 2(a) and 2(b)].

Values of θ_r obtained for a wide variety of IGA source conditions are shown in Fig. 3. Varying f significantly changes the cluster velocity⁵ but causes only small variations in cluster size [see Fig. 2(f)]. As long as $T_s \sim 290$ K, θ_r remains in the range $12^\circ - 18^\circ$ regardless of the temperature of the substrate [Fig. 3(a)—square symbols].¹⁷ Changing T_s causes a significant change in θ_r : for $T_s=77$ K, $\theta_r \sim 29^\circ$ [Fig. 3(a)—triangle symbols]; there is also a small change in mean cluster size, from $D_{av} \sim 30$ nm at $T_s=290$ K to $D_{av} \sim 22$ nm at $T_s=77$ K [Fig. 2(f)].

When the type of inert gas in the source was varied by replacing Ar with He ($T_s=290$ K), the resulting SEM images show a remarkable *sharp* transition from $\theta_r \sim 15^\circ$ to $\theta_r \sim 29^\circ$ [Figs. 2(c) and 2(d)]. θ_r is plotted as a function of $f_{\text{He}}/f_{\text{Ar}}$ in Fig. 3(b). Since the measured nanoparticle size [Fig. 2(f)—circles] does not exhibit a stepwise change during this sequence of experiments, we conclude that the change in θ_r occurs because of a change in *state* of the clusters. This is consistent with electron-diffraction experiments¹⁸ where changing the inert gas also caused clusters to change state. The change from small θ_r ($\sim 15^\circ$) to large θ_r ($\sim 29^\circ$) as clusters solidify is also consistent with the expectation that a liquid particle will deform more than a solid particle, increasing the area of contact with the substrate, dissipating more kinetic energy, and resulting in reduced rebound energy. Returning to Fig. 3(a), it is now clear that the change from $\theta_r \sim 29^\circ$ to $\theta_r \sim 15^\circ$ is consistent with the decrease in T_s (from 290 to 77 K): cooling the source reduces the inert-gas temperature, thus cooling the clusters, and changing their state from liquid to solid.

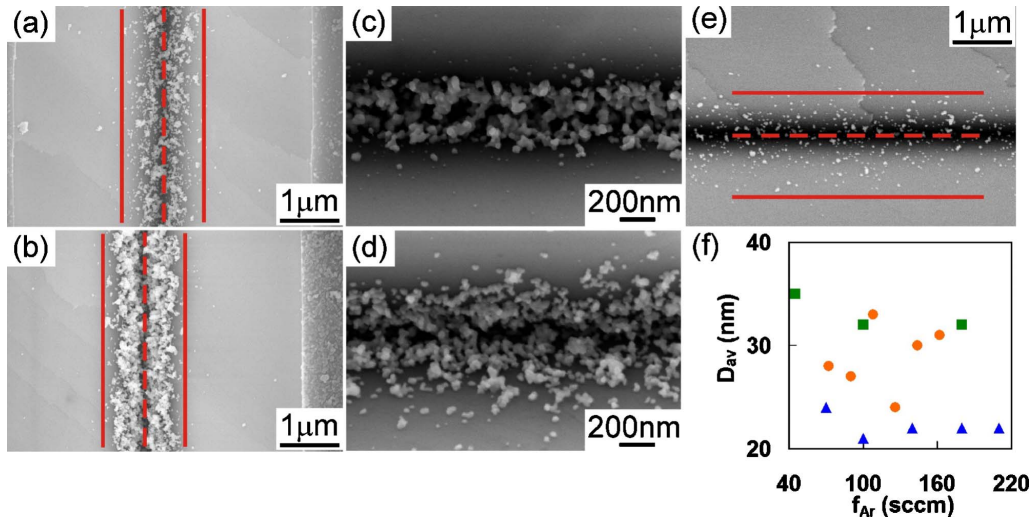


FIG. 2. (Color online) (a)–(e) Distribution of bismuth clusters in silicon V-grooves, which can be used to define the reflection angle θ_r . (a) and (b) Bi cluster distributions in $\sim 5 \mu\text{m}$ V-grooves for $f_{\text{Ar}}=100$ sccm and source and substrate temperatures $T_s=T_{\text{sub}}=290$ K. The clusters have bounced so that the upper V-groove walls support only a few clusters. The nominal mean cluster thickness was 2.4 nm in (a) and 7.2 nm in (b). The solid and dashed red lines mark the edge of the cluster distribution and the apex of the V-groove, respectively. (c) and (d) Bi cluster distributions deposited using a mixture of Ar and He inert gases at constant total flow rate: $f_{\text{He}}/f_{\text{Ar}}$ is 10% in (c) and 50% in (d). Again $T_s=T_{\text{sub}}=290$ K. The nominal mean cluster thickness was 5 nm. As discussed in the text, the increase in width of the cluster distribution corresponds to an increase in θ_r , which is due to a change in state of the clusters, from liquid to solid. (e) Cluster distribution when the sample was tilted by 15° in order to change the angle of incidence of the clusters. Deposition conditions were as for (a) and (b) but the nominal mean cluster thickness was 0.2 nm. The asymmetrical cluster distribution results from different angles of reflection on the two sides of the V-groove. (f) Mean cluster size (D_{av}) as a function of f_{Ar} . Squares: $T_s=290$ K; triangles: $T_s=77$ K; and circles: varying mixtures of Ar and He gas ($f_{\text{He}}+f_{\text{Ar}}=180$ sccm) and $T_s=290$ K. Note that the circles are scattered and do not show a monotonic dependence on $f_{\text{He}}/f_{\text{Ar}}$.

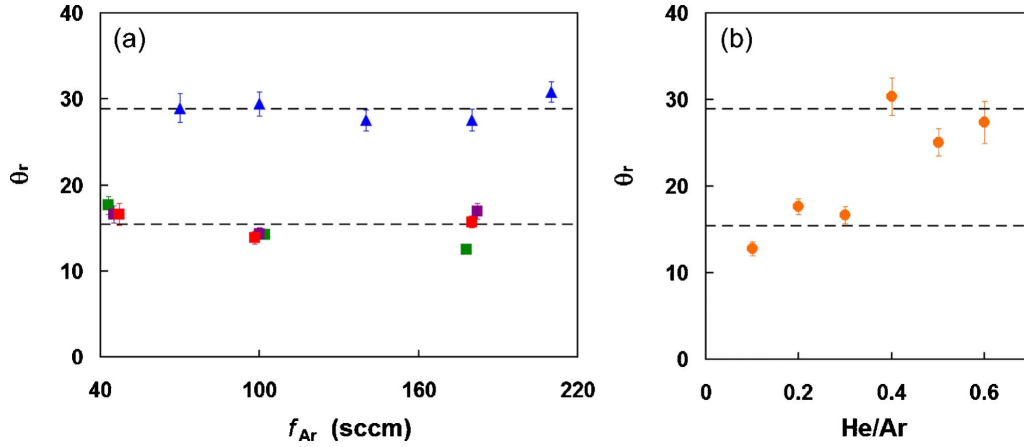


FIG. 3. (Color online) Rebound angles, θ_r , measured from depositions of Bi nanoparticles on etched silicon V-grooves. θ_r is estimated from the geometry of the V-groove and the width of the distribution of nanoparticles in the V-grooves. In each case, the nominal mean thickness of the deposition was 2 nm. (a) Squares represent depositions with $T_s=290$ K; the different colored squares are for different substrate temperatures, T_{sub} : green square 290 K; purple square 373 K; and red square 473 K. Triangles represent depositions with $T_s=77$ K. (b) The circles indicate θ_r for varying mixtures of Ar and He gases in the source chamber with total flow rate $f_{He}+f_{Ar}=180$ sccm and $T_s=T_{sub}=290$ K.

The normal coefficient of restitution can be calculated from θ_i and the measured values of θ_r ,

$$e_z = \frac{v_{fz}}{v_{0z}} = e_y \frac{\tan \theta_r}{\tan \theta_i}, \quad (1)$$

where the z direction is defined to be perpendicular to the surface of the V-groove and the y direction is parallel to the surface. Based on finite-element simulations¹⁹ and MD simulations,²⁰ the tangential coefficient or restitution, $e_y=v_{fy}/v_{0y}$, is typically expected to be slowly varying, and

we expect $e_y \sim 0.8$. However, since e_y is not known for the experiments, we report only the ratio e_z/e_y : for the liquid ($\theta_r \sim 15^\circ$) and solid ($\theta_r \sim 29^\circ$) clusters discussed above, $e_z/e_y \sim 0.38$ and $e_z/e_y \sim 0.79$, respectively.

IV. MOLECULAR-DYNAMICS SIMULATIONS

Extensive molecular-dynamics simulations using modified Lennard-Jones (LJ) potentials,²⁰ have been carried out for both liquid and solid 561-atom nanoparticles incident ob-

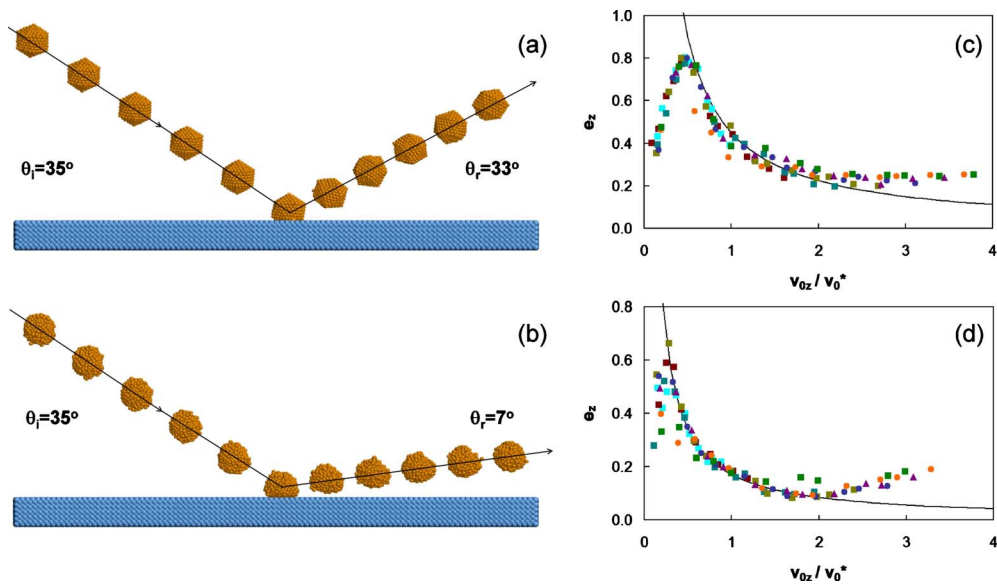


FIG. 4. (Color online) Snapshots from MD simulations of collisions of (a) solid and (b) liquid nanoparticles with a flat surface, at $\theta_i=35^\circ$ and $v_0=2.0v^*$. The reflection angle, θ_r , is smaller for the liquid particle because more energy is dissipated in the deformation of the particle and the deformed liquid particles adhere to the substrate more strongly. (c) and (d) normal coefficient of restitution, e_z , for simulated solid and liquid LJ nanoparticles, respectively (note the different vertical scales). Collisions were simulated for a wide range of angles of incidence and incident velocities (each symbol type represents a different θ_i), and e_z is calculated from v_{fz}/v_{0z} . The solid lines in (c) and (d) are power laws with a v_{0z}^{-1} dependence. Deviations from this dependence for $v_{0z} > 2$ are due to an increasing degree of fragmentation.

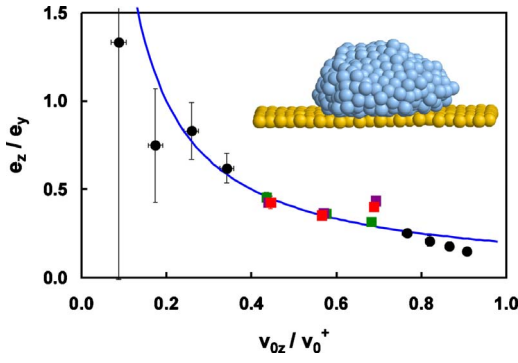


FIG. 5. (Color online) Experimentally determined normal coefficient of restitution, e_z , (normalized to the tangential coefficient of restitution, $e_y=0.8$ —see text) for Bi nanoparticles, as a function of the normal component of the incident velocity, v_{0z} (where $v_0^+=48$ m/s) (Ref. 23). The data were obtained with Ar as the inert gas and $T_s=290$ K, i.e., for liquid clusters. At small v_{0z} , it is difficult to estimate the position of the edge of the cluster distribution precisely, and so the uncertainty in e is substantial. At higher velocities, much of the data lies close to the solid blue curve, which is a v_{0z}^{-1} dependence. Circle data are for particles deposited at varying angles of incidence [see Fig. 2(e)]. In each case, the nominal mean thickness of the deposition was 0.2 nm. Square data are obtained from the reflection angle data in Fig. 3(a) for various v_0 and $\theta_i=35^\circ$. Inset: snapshot showing extensive plastic deformation in a simulated solid LJ particle with $v_0=3.8v^*$ and $\theta_i=35^\circ$.

liquely on planar surfaces,²¹ with the cluster-surface interaction parameter,²⁰ C , set to 0.2 [see Refs. 3 and 20 and Figs. 4(a) and 4(b)]. The velocities of the particles were varied between $0.1v^*$ and $4v^*$, where $v^*=(\epsilon/m)^{1/2}$ is the velocity in LJ units, and θ_i was varied between 15° and 90° . The reflection angle, θ_r , is found to be smaller for liquid particles because more energy is dissipated in the deformation of the particle. Typical values of e_z for liquid clusters are found to be roughly half the values found for solid clusters with the same velocity, in good agreement with the experiments discussed above.

Figures 4(c) and 4(d) show that values of e_z obtained as a function of v_{0z} , and for a wide range of θ_i , collapse onto separate master curves for the solid and liquid LJ clusters. For $v_{0z}\sim 0$, all particles stick and $e_z\sim 0$. The initial increase in e_z with v_{0z} is because the incident kinetic energy is sufficient for the particles to overcome their attraction to the surface and to rebound.

As the velocity increases further, the clusters are increasingly deformed on impact (see also Refs. 3 and 20), leading to a decrease in e_z . This decrease follows approximately a power-law dependence,

$$e_z \sim v_{0z}^{-p}, \quad (2)$$

where the exponent $p\sim 1$ for both the solid and liquid clusters. Focusing now on the solid clusters, the variation in e_z with v_{0z} is stronger than expected from either the Hertzian description¹⁴ ($p=1/4$) or finite-element simulations^{19,22} ($p=1/2$) of macroscopic systems. Although the yield stress is expected to be larger in nanoscale solid particles than in corresponding bulk materials,² these results show that once

the particles reach a velocity where they begin to yield, the increase in plastic deformation with impact velocity is much stronger than in the macroscopic case. The reason for this is apparent in snapshots of simulated solid particles [see Fig. 5 (inset)], which show that at high v_{0z} , the nanoparticles are plastically deformed^{3,20} over a significant part of their volume. Larger solid particles^{14,19,22} cannot undergo such an enormous degree of deformation and hence plastic deformation has a much more dramatic effect on the bouncing of nanoparticles. The inset of Fig. 5 (see also Refs. 3 and 20) shows that the mechanism of deformation is similar to the amorphization described in Ref. 2.

V. EXPERIMENTS AS A FUNCTION OF ANGLE OF INCIDENCE

By tilting the substrates in the experiments, it is possible to vary the angle of incidence, and hence the normal component of the incident velocity, v_{0z} . For each tilt angle, data can be obtained for two different angles of incidence: the width of the distribution on one face of the V-groove is correlated with the angle of reflection from the opposite face [see Fig. 2(e)]. For liquid clusters generated with $T_s=290$ K, θ_r ranges from $\sim 7^\circ$ to $\sim 18^\circ$ as θ_i is changed from 5° to 65° (there is large measurement uncertainty at small θ_i —see Fig. 5).

Given θ_r and θ_i , e_z/e_y can be calculated as a function of v_{0z} from Eq. (1), as shown in Fig. 5:²³ much of the data lies close to the solid blue curve, which represents a v_{0z}^{-1} dependence. For the highest velocities, the experimental data appear to fall off more quickly than v_{0z}^{-1} , which suggests even stronger plastic deformation.

VI. CONCLUSIONS

Comparison of Figs. 4 and 5 shows that, notwithstanding differences in particle size and difficulties comparing LJ parameters with parameters of real materials,³ the simulations and experiments yield very similar variations in e_z . The results, for both solid and liquid particles, are a consequence of the significant degree of deformation that occurs during impact at high velocities.

The strong plastic deformation at high v_{0z} is consistent with another experimental observation: particles incident on flat plateaus between V-grooves (with velocity v_0) are often observed to stick whereas the particles incident on the inclined walls of the V-groove (with $v_{0z}=v_0 \sin \theta_i$) bounce—see Figs. 2(a) and 2(b). This counterintuitive behavior occurs because the large deformation of the clusters on impact at $\theta_i=90^\circ$ leads to clusters sticking while at lower impact angles $v_{0z}<v_0$, less energy is dissipated in plastic deformation and the clusters bounce.

The present measurements and simulations of e are steps toward an understanding of the elastomechanical behavior of nanoparticles, which is needed for applications such as process engineering and filtration of nanoparticulates.¹¹ e is material dependent and so it is important that data are obtained for other particles and substrates, especially those which might be of concern from a health and safety standpoint.¹²

- *Present address: Department of Physics, United Arab Emirates University, Al Ain, United Arab Emirates.
- ¹Q. F. Gu, G. Krauss, W. Steurer, F. Gramm, and A. Cervellino, *Phys. Rev. Lett.* **100**, 045502 (2008).
 - ²H. Ikeda, Y. Qi, T. Cagin, K. Samwer, W. L. Johnson, and W. A. Goddard, *Phys. Rev. Lett.* **82**, 2900 (1999).
 - ³A. Awasthi, S. C. Hendy, P. Zoontjens, S. A. Brown, and F. Natali, *Phys. Rev. B* **76**, 115437 (2007).
 - ⁴W. Harbich, in *Metal Clusters at Surfaces*, edited by K.-H. Meiwes-Broer (Springer, Berlin, 2000), Chap. 4.
 - ⁵J. Partridge, S. A. Brown, A. D. F. Dunbar, M. Kaufmann, S. Scott, M. Schulze, R. Reichel, C. Seigert, and R. Blaikie, *Nanotechnology* **15**, 1382 (2004).
 - ⁶M. Hillenkamp, J. Pfister, M. Kappes, and R. Webb, *J. Chem. Phys.* **111**, 10303 (1999).
 - ⁷M. Hillenkamp, S. Jester, and M. Kappes, *J. Chem. Phys.* **116**, 6764 (2002).
 - ⁸V. Popok and E. Campbell, *Rev. Adv. Mater. Sci.* **11**, 19 (2006).
 - ⁹S. Pratontep, P. Preece, C. Xirouchaki, R. E. Palmer, C. F. Sanz-Navarro, S. D. Kenny, and R. Smith, *Phys. Rev. Lett.* **90**, 055503 (2003).
 - ¹⁰H. Haberland, Z. Insepov, and M. Moseler, *Phys. Rev. B* **51**, 11061 (1995).
 - ¹¹S. Sato, D. Chen, and D. Pui, *Aerosol and Air Quality Research* **7**, 278 (2007), and references therein.
 - ¹²A. Maynard, R. Aitken, T. Butz, V. Colvin, K. Donaldson, G. Oberdörster, M. Philbert, J. Ryan, A. Seaton, V. Stone, S. Tinkle, L. Tran, N. Walker, and D. Warheit, *Nature (London)* **444**, 267 (2006).
 - ¹³H. Wang and G. Kasper, *J. Aerosol Sci.* **22**, 31 (1991).
 - ¹⁴K. L. Johnson, *Contact Mechanics* (Cambridge University Press, UK, 1987).
 - ¹⁵R. Reichel, J. G. Partridge, A. D. F. Dunbar, S. A. Brown, O. Caughley, and A. Ayesh, *J. Nanopart. Res.* **8**, 405 (2006).
 - ¹⁶If the particles bounce again on the second impact, they will bounce either out of the V-groove (for $\theta_r=29^\circ$) or onto the upper surface of the V-groove (for $\theta_r=15^\circ$). The observed density of clusters is consistent with the amount of deposited material, and few clusters are observed on the upper surfaces of the V-groove, and so it is clear that the clusters bounce just once.
 - ¹⁷For large f_{Ar} , there is a small difference in θ_r for different substrate temperatures. The origin of this effect requires further investigation.
 - ¹⁸A. Wurl, M. Hyslop, S. Brown, B. Hall, and R. Monot, *Eur. Phys. J. D* **16**, 205 (2001).
 - ¹⁹C. Wu, C. Thornton, and L. Li, *Proc. R. Soc. London, Ser. A* **465**, 937 (2009).
 - ²⁰A. Awasthi, S. C. Hendy, P. Zoontjens, and S. A. Brown, *Phys. Rev. Lett.* **97**, 186103 (2006).
 - ²¹The solid and liquid clusters were equilibrated at temperatures $0.13\varepsilon/k_B$ and $0.65\varepsilon/k_B$, respectively, whereas the surface was equilibrated at $0.2\varepsilon/k_B$.
 - ²²C. Wu, L. Li, and C. Thornton, *Int. J. Impact Eng.* **28**, 929 (2003).
 - ²³Incident velocities are estimated from f , P_s , and the diameter of the source exit nozzle (see Ref. 1) and normalized to $v_0^+ = 48$ m/s for $f_{Ar}=100$ sccm and $\theta_i=90^\circ$. v_{0z} is then calculated from the angle of incidence on each of the two V-groove walls (see Fig. 1).